

Received Date : 28-Apr-2016
Revised Date : 20-Oct-2016
Accepted Date : 25-Oct-2016
Article type : Original Article

**The genetic architecture of novel trophic specialists:
higher effect sizes are associated with exceptional
oral jaw diversification in a pupfish adaptive
radiation**

CHRISTOPHER H. MARTIN¹, PRISCILLA A. ERICKSON², CRAIG T. MILLER²

¹Department of Biology, University of North Carolina at Chapel Hill, NC, USA

²Molecular and Cell Biology Department, University of California, Berkeley, CA, USA

Running Title: Quantitative trait loci in novel pupfish specialists

Key words: adaptive radiation, innovation, linkage mapping, novelty, diversification rate, ecological speciation, trophic divergence

Correspondence: Christopher H Martin. Department of Biology, University of North Carolina at Chapel Hill, Campus Box 3280, 120 South Rd., NC, 27599, USA

Email: chmartin@unc.edu

Data accessibility: All datasets used for this study will be deposited in Dryad. All Illumina reads sequenced will be deposited in the NCBI Short Read Archive.

This article has been accepted for publication and undergone full peer review but has not been through the copyediting, typesetting, pagination and proofreading process, which may lead to differences between this version and the Version of Record. Please cite this article as doi: 10.1111/mec.13935

This article is protected by copyright. All rights reserved.

Abstract

The genetic architecture of adaptation is fundamental to understanding the mechanisms and constraints governing diversification. However, most case studies focus on loss of complex traits or parallel speciation in similar environments. It is still unclear how the genetic architecture of these local adaptive processes compares to the architecture of evolutionary transitions contributing to morphological and ecological novelty. Here we identify quantitative trait loci (QTL) between two trophic specialists in an excellent case study for examining the origins of ecological novelty: a sympatric radiation of pupfishes endemic to San Salvador Island, Bahamas containing a large-jawed scale-eater and a short-jawed molluscivore with a skeletal nasal protrusion. These specialized niches and trophic traits are unique among over 2,000 related species. Measurements of the fitness landscape on San Salvador demonstrate multiple fitness peaks and a larger fitness valley isolating the scale-eater from the putative ancestral intermediate phenotype of the generalist, suggesting that more large-effect QTL should contribute to its unique phenotype. We evaluated this prediction using an F2 intercross between these specialists. We present the first linkage map for pupfishes and detect significant QTL for sex and eight skeletal traits. Larger-effect QTL contributed more to enlarged scale-eater jaws than the molluscivore nasal protrusion, consistent with predictions from the adaptive landscape. The microevolutionary genetic architecture of larger-effect QTL for oral jaws parallels the exceptional diversification rates of oral jaws within the San Salvador radiation observed over macroevolutionary timescales and may have facilitated exceptional trophic novelty in this system.

Introduction

A central problem in evolutionary biology is how genetic architecture constrains organismal diversification. Many theoretical and empirical studies have examined how standing variation, effect size, and pleiotropic effects of alleles may accelerate or impede adaptation and speciation (Schluter 1996; Orr 2005a; Stern & Orgogozo 2009; Kelly 2009; Wagner & Zhang 2011; Servedio *et al.* 2011; Rockman 2012). An emerging consensus among recent case studies is the repeated use of standing genetic variation for parallel adaptation to new environments, such as post-glacial lakes and streams (Colosimo *et al.* 2005; Rogers & Bernatchez 2007; Miller *et al.* 2007; Jones *et al.* 2012; Gagnaire *et al.* 2013), novel hosts (Feder *et al.* 2003), or lighter soils (Manceau *et al.* 2010). However, adaptation from standing variation is also frequently complemented by new mutations contributing to convergent evolution (Chan *et al.* 2010) and introgression among incipient species, which appears to be a pervasive feature of adaptive radiation (Rieseberg *et al.* 2007; Mims *et al.* 2010; Heliconius Genome Consortium 2012; Keller *et al.* 2013; Martin & Feinstein 2014; Huerta-Sánchez *et al.* 2014; Stankowski & Streisfeld 2015; Lamichhaney *et al.* 2015; Malinsky *et al.* 2015; Martin *et al.* 2015, 2016). Further consensus among these studies is that alleles of moderate to large effect play a role not only in human-mediated evolution (Orr 1999; Meyer & Purugganan 2013; Lemmon *et al.* 2014), but also rapid adaptation in natural populations (Albertson *et al.* 2003; Colosimo *et al.* 2004; Weber *et al.* 2013; Zhan *et al.* 2015) complemented by the expected exponential distribution of QTL effect sizes (Erickson *et al.* 2004; Albert *et al.* 2008; Wagner *et al.* 2008; Miller *et al.* 2014; but see Fishman *et al.* 2002).'

Within the growing number of case studies of speciation genomics it is still difficult to pinpoint specific architectures that constrain or promote speciation (e.g. Ortíz-Barrientos & Noor 2005); instead, common patterns of introgression and large-effect alleles in standing

variation are consistent with phenotypic studies which rarely find evidence of constraint in genetic or phenotypic variance-covariance matrices (Blows *et al.* 2004; Mezey & Houle 2005; Hine & Blows 2006; Agrawal & Stinchcombe 2009; Kirkpatrick 2009), artificial selection studies (Brakefield & Roskam 2006), or alignment between “genetic lines of least resistance” and phenotypic axes of diversification (Schluter 1996; McGuigan *et al.* 2005; Martin 2012). However, the repeated use of large-effect QTL during adaptation to new environments may provide some evidence of the limited availability of beneficial segregating alleles: if the supply of large-effect alleles is limiting, then these alleles should be more likely to be reused across similar environments. Recent studies did find a weak association between QTL effect size and shared QTL driven by a few loci across parallel speciation of stickleback (Conte *et al.* 2015; Erickson *et al.* 2016).

However, many of these case studies examined local adaptation or the repeated parallel evolution of similar ecotypes across similar environments. Furthermore, the majority of studies focus on loss of a complex trait and rarely examine gains of novel function within complex traits (Colosimo *et al.* 2004; Protas *et al.* 2006; Jeffery 2008; Chan *et al.* 2010; Glazer *et al.* 2014; but see Shapiro *et al.* 2013; Erickson *et al.* 2014; Arnegard *et al.* 2014; Cleves *et al.* 2014; Concannon & Albertson 2015). Therefore, it is still unclear how these microevolutionary processes scale up to morphological novelties, such as the evolution of novel adaptive zones or complex functional traits (Erwin 2000, 2015; Martin 2016).

A young sympatric adaptive radiation of *Cyprinodon* pupfishes on San Salvador Island, Bahamas is an excellent system to address these questions because two trophic specialist species within the radiation have rapidly adapted to novel ecological niches using complex functional traits (Martin & Wainwright 2011, 2013a). A specialized scale-eating

pupfish with greatly enlarged oral jaws (Fig. 1) evolved from an ancestral diet of algae scraping and microinvertebrates (common to all allopatric *Cyprinodon* outgroup taxa) within only 10,000 years and is endemic to hypersaline lakes on the 20-kilometer San Salvador Island (Martin & Wainwright 2011). Based on current natural history knowledge, this niche appears to be unique among over 2,000 related fish species and separated by 168 million years from the most closely related extant scale-eating specialists (Martin & Wainwright 2013b). This novelty index rivals nearly every other specialized niche observed during incipient adaptive radiation (Martin & Wainwright 2013b). The second specialist on San Salvador is a molluscivore with an enlarged nasal protrusion possibly functioning as a stabilizing wedge for shell-crushing (Fig. 1). Similarly, this novel appendage is unique among over 2,000 atherinomorph and cyprinodontiform fishes (Setiamarga *et al.* 2008; Martin & Wainwright 2013b). In many ways, these two trophic specialists exhibit opposing phenotypes to the third species in the radiation, the generalist *C. variegatus*, which is intermediate between the two specialists in nearly all aspects of its phenotype (Martin & Wainwright 2011, 2013a). The intermediate generalist phenotype is the putative ancestral founder of the radiation due to the nested position of the San Salvador clade within outgroup generalist populations distributed across the Caribbean with minimal variation in trophic morphology (Martin 2016b). The distinct skeletal morphologies of these specialists are heritable when reared in a common laboratory environment (Martin & Wainwright 2013c). Populations of these two species in Crescent Pond maintain substantial reproductive isolation ($F_{st} = 0.27$: Martin & Feinstein 2014) despite their sympatric breeding territories and inter-fertility in the laboratory.

This system provides an excellent opportunity to investigate the genetic architecture of major ecological transitions across trophic levels by the gain of complex and heritable adaptive trophic morphology within young species that are amenable to laboratory crosses.

Furthermore, exceptional rates of trophic diversification in this clade reach up to 51 times faster than diversification rates in allopatric *Cyprinodon* species (Martin & Wainwright 2011) and can be placed in the context of field measurements of the fitness landscape on San Salvador from the growth and survival of F2 hybrids (Martin & Wainwright 2013c; Martin 2016). Knowledge of fitness peaks and valleys in this system enables explicit tests of the predicted distribution of effect sizes for adaptation to new adaptive peaks (Orr 2005b). Fitness measurements demonstrate that the molluscivore has colonized a novel fitness peak separated by a fitness valley from the generalist ancestral phenotype and that an even larger fitness valley isolates the scale-eater phenotype from other species (Fig. 2; Martin & Wainwright 2013c; Martin 2016a). Based on the different-sized fitness valleys isolating these two specialist phenotypes, we predict that more large-effect alleles will underlie the scale-eater phenotype (i.e. larger jaw size) than the molluscivore phenotype (nasal protrusion). This prediction is based on Orr's extension of Fisher's geometric model of adaptation: large-effect alleles are more likely to be beneficial early in adaptive walks than small-effect alleles (i.e. larger phenotypic effects are more likely to move a population closer to a fitness optimum when the population is far away from that optimum) and thus are more likely to be fixed in a population (Orr 1998, 2005a). By extension, we expect an increased frequency of larger-effect alleles in populations crossing larger fitness valleys. We define 'large-effect' as QTL explaining more than 20% of trait variance; 'moderate-effect' as QTL explaining 10-20% of trait variance; and 'small-effect' as QTL explaining less than 10% of trait variance.

Here, we provide the first investigation of genetic architecture in pupfishes, focusing on the two ecologically and morphologically novel specialist species on San Salvador. We construct the first pupfish linkage map and map QTL associated with eight skeletal traits and sex determination. Based on our measurements of the fitness landscape in this system (Fig.

2), we test our prediction that adaptation to scale-eating should involve larger-effect QTL than adaptation to molluscivory. Investigating the origins of trophic innovations, such as scale-eating, complements studies of local adaptation and repeated parallel evolution and enables comparisons of how genetic architecture shapes the rare evolution of major ecological and morphological novelty during nascent adaptive radiation.

Methods

Genetic Cross

Wild-caught individuals of the scale-eating pupfish *C. desquamator* (Martin & Wainwright 2013a) and the molluscivore pupfish *C. brontotheroides* (Martin & Wainwright 2013a) were collected from Crescent Pond, San Salvador Island, Bahamas using a handheld net while snorkeling. A single wild-caught female *C. desquamator* was allowed to naturally breed with a single wild-caught male *C. brontotheroides* in a 40-liter aquarium on synthetic spawning mops. Four F1 hybrids were crossed to each other within a single 40-liter aquarium to generate the F2 intercross over the course of approximately one year, resulting in 190 F2 individuals genotyped for this study. A subset of these individuals could be identified as males by their breeding coloration; juveniles and females display similar coloration and females were identified by lack of breeding coloration above adult size (but note that some misidentification of the female sex may occur). All fish were reared in a common laboratory environment at the University of California, Davis at 5-10 ppt salinity, pH 8.3, 25-28° C. Fry were initially raised on newly hatched *Artemia* nauplii for the first 40 days post-fertilization, followed by mixed frozen and pellet foods. All fish were euthanized in an overdose of buffered MS-222 (Finquel, Inc.) following approved University of California, Davis Institutional Animal Care and Use Protocol #17455 and preserved in 95% ethanol.

Phenotyping

C. desquamator and *C. brontotheroides* share the same benthic habitat within Crescent Pond, but exhibit highly divergent trophic morphology and overall body shape (Fig. 1; Martin & Wainwright 2011). The scale-eating pupfish, *C. desquamator*, is defined by the proportionally largest oral jaws among over 200 species within Cyprinodontidae, enlarged adductor muscles, and reduced body depth for performing rapid high-speed biting strikes to remove scales from nearby pupfish. Scales and their associated protein-rich mucus layer comprise approximately 50% of its diet in Crescent Pond (Martin & Wainwright 2011, 2013a). The molluscivore pupfish, *C. brontotheroides*, is defined by a maxillary nasal protrusion surrounding the upper jaw, a unique trait among over 2,000 Cyprinodontiform fishes and short, robust oral jaws with a large closing in-lever to increase mechanical advantage for crushing gastropods and ostracods, which make up about 30% of its diet in Crescent Pond (Martin & Wainwright 2013b).

We used clearing and double-staining with alizarin red and alcian blue to measure skeletal phenotypes in the F2 hybrids. Each specimen was fixed in 95% ethanol and skinned. Specimens were then soaked in 5% buffered formalin and stained following the protocol described in (Dingerkus & Uhler 1977). Cleared specimens were suspended in glycerin and photographed on both the left and right lateral sides at a focal distance framing the entire head and pectoral girdle in detail (Fig. 3) with a Canon EOS 60D digital SLR with a 60mm macro lens mounted on a tripod. The jaw was manually adducted in each photograph with a pin for a clear view of the quadroarticular region (Fig. 3a). A whole body photograph was also taken for fin and body measurements (Fig. 3b). We used tpsdig2 software (Rohlf 2001) to digitize a total of 19 landmarks on each lateral skull image and 12 landmarks on each whole body image plus a calibration distance of 4 mm in each photograph. Landmarks were

Accepted Article

calibrated and converted to 30 linear distances defining functional traits and the most divergent traits between the two San Salvador specialists (Fig. 3; supplemental methods). The mean trait distance was taken from each lateral skull image to reduce measurement error due to lateral positioning. In some cases, damage to skeletal features precluded measurement and one or both measurements were excluded. Each trait was strongly associated with specimen size and was individually size-corrected using the residuals from the linear regression of log-transformed trait on log-transformed standard length (SL). No QTL were detected for SL (Table 1).

Computed microtomography scans

To visualize skeletal features of each parental species in detail (Fig. 1), whole specimens of each specialist species preserved in 95% ethanol were scanned at the UNC Biomedical Research Imaging Center using a SCANCO μ CT40 (Brüttisellen, Switzerland) at 70 kVp, 114 μ A, 300 ms, 1000 projections, and down-sampled to a voxel size of 30 μ m. Scans were processed into surface volumes for each fish and output as .stl files using ImageJ (Schindelin *et al.* 2012) for visualization within MeshLab (meshlab.sourceforge.net).

Genotyping

F2 hybrids and their grandparents were genotyped using double-digest restriction site associated sequencing (ddRADseq) following (Peterson *et al.* 2012), with slight modifications described in previous studies (Martin *et al.* 2015, 2016). Four indexed libraries containing 96 barcoded individuals each were pooled and sequenced to 100-bp in single-end high-output mode on one lane of Illumina HiSeq 2000 and one lane of Illumina HiSeq 4000. One additional library of 47 samples was prepared separately, pooled with a previous study ($n = 96$ samples total; Martin *et al.* 2016), and sequenced on one lane of Illumina HiSeq 2000.

The two grandparents of the F2 cross were sequenced in two separate HiSeq 2000 lanes and pooled with previous studies (Martin & Feinstein 2014; Martin *et al.* 2016) in order to avoid lane-specific sequencing errors during genotyping. All lanes were sequenced at the Vincent J. Coates Genomic Sequencing Laboratory, California Institute for Quantitative Biosciences.

178.5 million 100-bp raw reads were sequenced across the four indexed F2 hybrid libraries in the first HiSeq2000 lane, 299.1 million reads in the HiSeq4000 lane, and 154.6 million total reads for the 47 samples pooled with a previous study (out of 96) in one HiSeq2000 lane for a total of 553.3 million reads. Raw reads were inspected using FastQC (Babraham Bioinformatics Institute) to inspect read qualities and trimmed using Trim Galore! (Babraham Bioinformatics Institute) to remove trailing bases below a Phred quality score of 20 ($\geq 1\%$ error rate). Trimmed reads were demultiplexed and quality filtered using the default settings in process_radtags (v. 1.35) from the Stacks pipeline (Catchen *et al.* 2013). Initial inspection indicated that approximately half of the barcoded reads were discarded due to a single base-pair substitution in the 8 base-pair SbfI restriction site motif, CCTGCAGG, which frequently appeared as CCTGCAGC or CCTGCACG, and were discarded due to lack of a perfect match to the restriction site by process_radtags. This may be due to increased star activity (i.e. off-site cleavage) by the SbfI restriction enzyme despite our use of the high-fidelity enzyme. To retain these additional RAD loci, we reran the process_radtags script with the `-disable_rad_check` flag enabled to prevent discarding reads with imperfect matches to the restriction site. Filtered reads still required the 4-8 base pair molecular barcode sequence in order to be retained for downstream processing. Quality-filtered and demultiplexed reads were then aligned to the *Cyprinodon* reference genome assembly (v. 1.0, 1035 Mb, 81x coverage, NCBI: Wesley Warren, Grant ID 8 R24 OD011198-02) using BWA-MEM (Li 2013) under default settings. Aligned reads from each grandparent sequenced in

separate lanes were merged using Samtools (Li *et al.* 2009). A total of 330.8 million reads were aligned.

We used the Stacks pipeline (Catchen *et al.* 2013) to genotype aligned reads. A minimum of 3 identical aligned reads was required to define a RAD locus within each individual. Next, a catalog of all loci in both grandparents was built, detecting a total of 24,948 SNPs across 59,589 RAD loci. Homologous loci across F2 intercross individuals were determined by their genomic position (-g). Using a likelihood model which takes into account variation across individuals, SNPs within each F2 intercross individual were called only if present in the grandparent catalog, following Catchen *et al.* (2011). Loci with a minimum of six aligned reads were exported in generic format using the genotypes script (v. 1.35) with automated error correction enabled. Initial analyses exporting fewer high-coverage markers with a minimum read depth of 15 used to construct a linkage map in R/qtl robustly identified the same moderate-effect QTL for oral jaw size.

Linkage Map Construction

Genotypes were imported into R/qtl (v. 1.38-4, Arends *et al.* 2010) for initial filtering. Only homozygous markers fixed in each grandparent (aa/bb) were retained for analyses. Individuals genotyped at fewer than 10 loci and loci genotyped in fewer than 50 individuals were excluded, resulting in the final set of 190 individuals. Markers exhibiting significant segregation distortion ratios exceeding $P = 0.01$ (χ^2 test) were also excluded. This resulted in a filtered dataset of 420 markers in 190 F2 individuals each genotyped at 36.7% of markers on average. Genotype frequencies were 26.4% AA, 45.7% AB, 27.8% BB. These data were imported into JoinMap 4 (Van Ooijen 2006) for linkage map construction by regression mapping. The Haldane mapping function was used with the following parameters: linkages

with a recombination frequency smaller than 0.4 and a logarithm of odds (LOD) larger than 1.0, a goodness-of-fit jump threshold for removal of loci of 5.0, and a ripple performed after each added locus. Markers were assigned to linkage groups using LOD score 5 groupings. The first map was chosen for each linkage group without using multiple passes to force additional markers. Four singleton markers were excluded. This map was exported to R/qtl for analyses ($n = 416$ markers).

QTL analysis

QTL were mapped for 30 skeletal traits and sex using R/qtl (v. 1.38-4, Arends *et al.* 2010) in the R programming environment (R Core Team 2015). Genotype probabilities were calculated from 1000 permutations using a step size of 1 and an error probability of 0.01.

Haley-Knott regression was used in a first pass to detect significant QTL using a genome-wide significance threshold of $P < 0.05$ from 1000 permutations using the function *scanone*.

Next, significant QTL were re-evaluated using maximum likelihood (EM algorithm: Lander and Botstein 1989) and multiple imputation models (Sen and Churchill 2001). Maximum likelihood genome-wide significance thresholds were evaluated for each trait based on 1000 permutations. The *stepwiseqtl* function was then used to explore models with up to four interacting QTL for each trait. The best-fitting qtl model was refined using the *fitqtl* and *refineqtl* functions in order to estimate the proportion of variance explained and the P -value of each significant QTL. A 95% Bayesian credible interval was estimated for significant QTL from the maximum likelihood model using the *baysint* function in Rqtl. The *plotPXG* function was used to plot phenotypes at specific markers. We evaluated potential epistasis among traits using the *scantwo* function under the maximum likelihood model and visualized all two-way trait interactions for premaxilla length, which displayed the most significant QTL detected, and sex. We assessed significance of two-way interactions from 1000 permutations

for the full and interaction models using Haley-Knott regression. We used the *qtlDesign* package in R to estimate the power of our sample size and marker coverage to detect QTL (Sen *et al.* 2007).

Results

Linkage Map Construction

We identified 29 linkage groups from 416 markers (Fig. S1), slightly higher than the 24 haploid chromosomes estimated from karyotypes of several *Cyprinodon* species (Stevenson 1981; Liu & Echelle 2013). The only known exceptions to this rule within Cyprinodontidae are the closest outgroup *Megupsilon* and another closely related outgroup *Garmanella*, each with an independent sex-linked chromosomal fusion resulting in $2n = 47$ in males (Collier *et al.* 2016; also see Pennell *et al.* 2015 for a review of this pattern in fishes). With additional markers, we anticipate that the true number of linkage groups is also 24 in San Salvador Island *Cyprinodon*. The total map length was 1458 cM with no linkage group spanning more than 110 cM and no inter-marker map distance greater than 25 cM, indicating a robust map comparable to other recent linkage mapping studies using RADseq (Hohenlohe *et al.* 2010; Barchi *et al.* 2012; Hecht *et al.* 2012; Recknagel *et al.* 2013; O'Quin *et al.* 2013; Gagnaire *et al.* 2013; Franchini *et al.* 2014; Yong *et al.* 2016).

Significant QTL

We detected significant QTL for eight skeletal traits and sex that map to five different linkage groups (Table 1; Fig. 4-6, S2-S3). The eight skeletal traits mapped to linkage groups 2, 8, 9 or 15 and sex mapped to linkage group 1 (Fig. 4). Sex was not perfectly associated with the QTL peak marker and in 5 individuals sex was discordant (Fig. 5), possibly indicating polygenic sex determination and/or misidentification of phenotypic sex. Within the subset of

fish identified as males with strong confidence (females exhibit juvenile coloration and may be confused with juvenile males), there were all possible genotypes at the peak QTL marker, consistent with a complex sex determination system. Linkage group 15 was associated with all four measured aspects of oral jaw size, specifically both the length and width of the upper and lower jaws (Fig. 4). This consistency across four different oral jaw traits provides additional support for one or more genomic regions on this linkage group contributing to differences in overall jaw size. This clustering may reflect a single pleiotropic locus or a cluster of loci associated with jaw size spaced across this chromosome. The latter scenario is supported by only partial overlap of the LOD profiles and 95% Bayesian credible intervals for different oral jaw traits which centered on different regions of linkage group 15 (Fig. S3).

Interestingly, QTL for palatine height and height of the coronoid process of the articular each mapped to linkage group 8 and are spatially adjacent structures (Fig. 4) but are often grouped in different functional modules (oral jaw closing in-lever versus height of the craniofacial region). Finally, QTL acted in the same direction as the divergence observed between the parental species for all four oral jaw traits, opening in-lever, and palatine height, providing further support for QTL in these regions (Fig. 5). Cranial height and caudal peduncle height were divergent in heterozygotes, but not between parental genotypes (Fig. 5), which may reflect a past history of stabilizing selection on these traits (Albertson *et al.* 2003). All other traits exhibited a general pattern of additive inheritance (Fig. 5). We found no evidence of significant two-way interactions between QTL affecting oral jaw size (upper jaw length) or sex (Fig. S4).

Multiple QTL were not detected for any trait, most likely due to low sample sizes. Given our linkage map and sample size of 190 individuals, we caution that our analysis was only able to detect significant QTL ($\alpha = 0.05$) for effect sizes greater than 10.8% PVE with 80% power, 7.6% PVE with 50% power, and 5.8% PVE with 30% power. Thus, we had a high chance of detecting moderate-effect and large-effect QTL, but limited power to detect small-effect QTL.

However, interesting trends were observed for some non-significant LOD peaks. The second and third highest peak LOD scores for premaxilla length on linkage groups 6 and 8 were also observed as the third and fourth highest peak LOD scores on the same two linkage groups for lower jaw length (Fig. 4a,c). The second highest LOD score for lower jaw length corresponded to linkage group 4 and this linkage group also showed elevated association with premaxilla length (Fig. 4a,c). Combined, these observations are consistent with 3-4 moderate-to-small effect QTL affecting variation in oral jaw size between these specialists. Furthermore, many QTL were associated with linkage group 15, including all oral jaw traits measured but also non-significant trends of association for nasal tissue protrusion and maxilla length (Fig. S2), suggesting the buildup of adaptive substitutions in this region.

Larger effect sizes predicted for larger fitness valleys

To visually assess whether our data were consistent with the hypothesis that adaptation to the more distant scale-eating fitness peak across a longer, deeper fitness valley should more often use larger effect alleles than adaptation to the molluscivore fitness peak across a shorter, shallower fitness valley (Fig. 2: based on previous phenotypic analyses in (Martin & Wainwright 2011, 2013c; Martin 2016a), we contrasted effect sizes between the most distinctive scale-eater and molluscivore traits (Figs. 4-6). Lower and upper jaw length were

most divergent in the scale-eating species and corresponded to the largest QTL effect sizes observed in this study (Figs. 4-6, Table 1). These QTL were all positive in direction in the scale-eater (Fig. 5), increasing jaw size from the putative ancestral intermediate jaw sizes of the generalist *C. variegatus*. In contrast, nasal protrusion distance and angle were most divergent in the molluscivore species and measurements of maxillary head protrusion and nasal tissue protrusion did not map to any significant QTL (Fig. 6, S2, Table 1). Overall, our novel visualization of effect sizes across measured skeletal traits in this cross suggests that the largest QTL effect sizes are concentrated in the oral jaws (Fig. 6), consistent with the defining phenotype of the scale-eater (Martin & Wainwright 2013a) and the major axis of trophic diversification in this radiation (Martin & Wainwright 2011; Martin 2016b).

Discussion

We examined the genetic architecture of trophic morphology within an incipient adaptive radiation of pupfishes on San Salvador. This system provides an interesting contrast to many other case studies of incipient speciation because this radiation is spatially restricted to a single island despite abundant comparable habitats (Martin 2016b) and it shares features with older, classic examples of adaptive radiation (Fryer & Iles 1972; Schluter & Grant 1984; Givnish *et al.* 1997; Kocher 2004; Gavrillets & Losos 2009; Reding *et al.* 2009; Martin & Genner 2009; Harmon *et al.* 2010; Martin 2010, 2013; De León *et al.* 2014; Pfaender *et al.* 2016), such as rapid diversification rates (Martin and Wainwright 2011), novel ecological niches spanning trophic levels (Martin & Wainwright 2013b), variable progress toward speciation (Martin & Feinstein 2014), and a complex adaptive landscape with multiple fitness peaks (Fig. 2; Martin & Wainwright 2013c; Martin 2016). We present the first linkage map and quantitative genetic analyses of trophic morphology and sex determination within *Cyprinodon* pupfishes (Fig. 3-6). This study is still one of few to examine the genetic

architecture of complex traits in a vertebrate with known fitness effects in the wild (but see Barrett *et al.* 2008; Ellegren & Sheldon 2008; Linnen *et al.* 2013; Arnegard *et al.* 2014; Lamichhaney *et al.* 2016) and adds to an emerging case study of the rare evolution of novelty during incipient adaptive radiation.

Moderate-effect QTL used for increased scale-eater jaw size

We found QTL for a reasonably large proportion of traits (8 out of 30 traits examined: Table 1), despite our low sample size ($n = 190$), and thus low power to detect QTL, indicating a number of moderate-effect QTL within this cross (i.e. QTL explaining 10-20% of phenotypic variation). Four of the QTL with the largest effect sizes, explaining up to 15% of trait variance (Table 1), were associated with oral jaw size and mapped to several regions of linkage group 15 (Fig. 4-5, S3). Additional suggestive but non-significant LOD peaks (LOD > 2.5) may indicate that three to four moderate-effect or small-effect QTL contributed to differences in overall jaw length. Elongated oral jaws are the main feature differentiating scale-eating pupfish from other species on San Salvador and, indeed, all other Cyprinodontidae (Martin & Wainwright 2013a). Jaw length loads heavily on the major discriminant axis and first principal component axis of phenotypic variation within this radiation (Martin & Wainwright 2011, 2013a; c). In contrast, no significant QTL were detected for the distinctive nasal protrusion of the molluscivore (Fig. 4, S2; Table 1). These observations are consistent with Orr's extension of Fisher's geometric model: larger-effect alleles facilitate crossing larger fitness valleys and reaching distant optima (Orr 1999, 2005b). This prediction is supported by prior measurements of the fitness landscape on San Salvador indicating that scale-eaters are separated by a larger fitness valley than molluscivores from their ancestral generalist peak (Fig. 2; Martin & Wainwright 2013c).

Limitations and future directions

Although our results are consistent with Orr's extension of Fisher's geometric model applied to specialists crossing different-sized fitness valleys, they do not offer a sufficient test. Ideally, the distribution of QTL would be estimated from a larger sample of F2 hybrids generated from two separate F2 intercrosses: one for each specialist species crossed to the generalist, the putative ancestral phenotype of the founding population of San Salvador (based on the nested position of the San Salvador radiation within outgroup generalist populations throughout the Caribbean: Martin and Wainwright 2011; Martin 2016b). However, due to the consistent intermediate phenotypic position of the generalist relative to the extreme and opposing phenotypes of the two specialist species in our cross, we can make predictions about which QTL might be relevant to crossing these respective fitness valleys based on the sign of the QTL and the distribution of phenotypes in the parental specialist species. For example, moderate-effect QTL likely increased jaw length toward the scale-eater phenotype relative to the intermediate jaw size of the generalist (Fig. 5); in contrast, no QTL were detected for nasal protrusion (Table 1), indicative of small effect sizes undetectable by our small sample size. Future studies with larger samples of F2 fish, as well as denser genetic markers, will further test the genetic architecture of pupfish trophic specialization, as well as ultimately consolidate the linkage map (with the number of linkage groups equal to the number of chromosomes). Nonetheless, it is important to note that our lack of power to estimate the distribution of QTL effect sizes limits our ability to test Orr's model. Furthermore, such distributions of QTL effect sizes may differ in future crosses between the specialists and generalist due to epistasis and phenotypic plasticity. For example, QTL for skeletal morphology can almost completely differ within a cichlid cross raised in different foraging environments in the laboratory (Parsons *et al.* 2016). This result may be due to the marked difference in trophic plasticity between the relatively divergent cichlid species used

in this cross (different trophic guilds spanning over 20 closely related species) resulting in segregating genetic assimilation loci (Parsons *et al.* 2014), which may be a relatively rare phenomenon (Levis & Pfennig 2016; Martin *et al.* 2016). Although the trophic morphology of pupfish specialists is heritable over multiple generations in the laboratory and exhibits minimal phenotypic plasticity (Martin & Wainwright 2013c), the fitness of QTL and adaptive trophic morphology in the wild, rather than laboratory-reared colonies, is most relevant to adaptive diversification (e.g. Korves *et al.* 2007; Ferris *et al.* 2016).

Our study adds to a growing literature examining the genetic architecture of adaptation to new fitness peaks (Bratteler *et al.* 2006; Gifford *et al.* 2011; Louthan & Kay 2011; Rogers *et al.* 2012). A recent review predicted that “at least one large effect mutation is required” for adaptation to multiple fitness optima, but did not consider fitness regimes more complex than disruptive selection (Dittmar *et al.* 2016). Our results are consistent with the general observation that the topography of the fitness landscape is likely to affect the effect size distribution of adaptive substitutions (Orr 1998, 2005a; Matuszewski *et al.* 2015; Dittmar *et al.* 2016).

Microevolutionary genetic architecture parallels patterns of macroevolutionary jaw diversification

QTL effect sizes mirrored patterns of rapid morphological diversification of the oral jaws on San Salvador relative to other pupfish species (Martin & Wainwright 2011; Martin 2016b). This pattern was mainly driven by the moderate effects of QTL for oral jaw size, but other moderate-effect QTL, such as jaw closing in-lever, also exhibited faster diversification rates in these phylogenetic comparative studies. Effect sizes were overestimated due to our small sample size (Beavis 1998); however, this bias should not affect relative differences in effect

Accepted Article

size among traits and genotyping rates were comparable across the eight QTL detected (Fig. S4). Phenotypic divergence is confounded with the overall detection probability for significant QTL underlying the phenotype; however, no significant QTL were detected for the highly divergent nasal protrusion phenotype of the molluscivore. Overall, this pattern is intriguing because it links microevolutionary estimates of genetic architecture to macroevolutionary diversification observed during adaptive radiation in the wild (also see Roberts *et al.* 2011).

The potential association between moderate effect sizes and faster diversification rates may be causative in either direction. Strong divergent selection over time may incrementally build up larger-effect haplotypes from many new mutations or recombination among existing haplotypes (Yeaman & Whitlock 2011). Alternatively, moderate-effect standing variation for jaw size in the ancestral population may have facilitated the evolution of scale-eaters and molluscivores along genetic lines of least resistance (Schluter 1996). In the latter scenario, faster diversification rates are expected because there is no waiting time for the buildup of small-effect mutations. Thus, we speculate that standing variation may have facilitated rapid diversification toward novel fitness peaks in this radiation. However, the rarity of the scale-eating pupfish and their endemism to a single tiny island in the Caribbean begs the question of whether the relevant standing variation exists in the many neighboring islands with ecologically similar hypersaline lakes (Martin 2016b). Despite extensive surveys, we are aware of only one other generalist pupfish population in Lake Cunningham, New Providence Island, Bahamas that exhibits increased jaw variation, but without the distinctive reproductive coloration, diet, or extreme jaw elongation observed on San Salvador (Martin pers. obs.; Turner *et al.* 2008).

Conclusion

We provide the first investigation of genetic architecture within a promising system for studying the origins of adaptive radiation and the evolution of novel trophic specialization. Based on previous measurements of a complex fitness landscape, we present preliminary estimates of QTL effect size suggestive of the quantitative genetic prediction that larger-effect QTL are more likely to be used to cross larger fitness valleys. We also highlight an intriguing parallel between phylogenetic diversification rates and QTL effect sizes, consistent with the hypothesis that genetic architecture promoted the observed patterns of phenotypic divergence in this radiation. Finally, we present a novel approach to visualizing this information on a ‘morphogram’ illustrating QTL effect sizes across the skeletal anatomy of *Cyprinodon*. These QTL and the first pupfish linkage map provide important resources for future genomic analyses in this group.

Acknowledgements

This study was funded by the Miller Institute for Basic Research in the Sciences, the Achievement Rewards for College Scientists Program, and a student grant from the Gerace Research Centre to CHM. I thank the Gerace Research Centre for accommodation and the Bahamian government for permission to conduct this research. R. Hanna assisted with permit applications and logistics. We thank the Vincent J. Coates Genomics Sequencing Laboratory at UC Berkeley, supported by NIH S10 Instrumentation Grants S10RR029668, S10RR027303 and OD018174, and the Small Animal Imaging Core facility at the UNC Biomedical Imaging Research Center, supported by an NCI cancer center grant #P30-CA016086-35-37. PAE was supported by NIH Predoctoral Training Grant #5T32GM007127. The authors declare no conflict of interest.

Data Accessibility

All datasets used for this study are deposited in Dryad: 10.5061/dryad.mn8k0, including genotype and phenotype matrices and scripts used for the Stacks pipeline. Genetic marker IDs, sequences, and scaffold IDs are included as supplemental material.

References

- Agrawal AF, Stinchcombe JR (2009) How much do genetic covariances alter the rate of adaptation? *Proceedings. Biological sciences / The Royal Society*, **276**, 1183–91.
- Albert AYK, Sawaya S, Vines TH *et al.* (2008) The genetics of adaptive shape shift in stickleback: pleiotropy and effect size. *Evolution; international journal of organic evolution*, **62**, 76–85.
- Albertson RC, Streelman JT, Kocher TD (2003) Directional selection has shaped the oral jaws of Lake Malawi cichlid fishes. *Proceedings of the National Academy of Sciences of the United States of America*, **100**, 5252–7.
- Arends D, Prins P, Jansen RC, Broman KW (2010) R/qtl: High-throughput multiple QTL mapping. *Bioinformatics*, **26**, 2990–2992.
- Arnegard ME, McGee MD, Matthews B *et al.* (2014) Genetics of ecological divergence during speciation. *Nature*, **511**, 307–311.
- Barchi L, Lanteri S, Portis E *et al.* (2012) A RAD tag derived marker based eggplant linkage map and the location of QTLs determining anthocyanin pigmentation. *PloS one*, **7**, e43740.
- Barrett RDH, Rogers SM, Schluter D (2008) Natural selection on a major armor gene in threespine stickleback. *Science (New York, N.Y.)*, **322**, 255–7.
- Beavis W (1998) QTL analyses: power, precision, and accuracy. In: *Molecular dissection of complex traits*, pp. 145–162.

- Blows MW, Chenoweth SF, Hine E (2004) Orientation of the genetic variance-covariance matrix and the fitness surface for multiple male sexually selected traits. *The American Naturalist*, **163**, 329–40.
- Brakefield PM, Roskam JC (2006) Exploring evolutionary constraints is a task for an integrative evolutionary biology. *The American Naturalist*, **168**, S4–S13.
- Bratteler M, Lexer C, Widmer A (2006) Genetic architecture of traits associated with serpentine adaptation of *Silene vulgaris*. *Journal of Evolutionary Biology*, **19**, 1149–1156.
- Catchen JM, Amores A, Hohenlohe P, Cresko W, Postlethwait JH (2011) Stacks: building and genotyping loci de novo from short-read sequences. *G3*, **1**, 171–82.
- Catchen J, Hohenlohe PA, Bassham S, Amores A, Cresko WA (2013) Stacks: an analysis tool set for population genomics. *Molecular Ecology*, **22**, 3124–40.
- Chan YF, Marks ME, Jones FC *et al.* (2010) Adaptive evolution of pelvic reduction in sticklebacks by recurrent deletion of a *Pitx1* enhancer. *Science (New York, N.Y.)*, **327**, 302–5.
- Cleves P a, Ellis N a, Jimenez MT *et al.* (2014) Evolved tooth gain in sticklebacks is associated with a cis-regulatory allele of *Bmp6*. *Proceedings of the National Academy of Sciences of the United States of America*, **111**, 13912–7.
- Collier GE, Echelle AA, Valdéz-González A (2016) Karyotypes of *Cualac tessellatus* and *Floridichthys carpio* : comments on the phylogenetic distribution of multiple sex chromosomes in North American cyprinodontids. *The Southwestern Naturalist*, **61**, 142–145.
- Colosimo PF, Hosemann KE, Balabhadra S *et al.* (2005) Widespread parallel evolution in sticklebacks by repeated fixation of *Ectodysplasin* alleles. *Science (New York, N.Y.)*, **307**, 1928–1933.

- Colosimo PF, Peichel CL, Nereng K *et al.* (2004) The genetic architecture of parallel armor plate reduction in threespine sticklebacks. *PLoS Biology*, **2**, E109.
- Concannon MR, Albertson RC (2015) The genetic and developmental basis of an exaggerated craniofacial trait in East African cichlids. *Journal of Experimental Zoology Part B: Molecular and Developmental Evolution*, **324B**, 662–670.
- Conte GL, Arnegard ME, Best J *et al.* (2015) Extent of QTL reuse during repeated phenotypic divergence of sympatric threespine stickleback. *Genetics*, **201**, 1189–1200.
- Dingerkus G, Uhler LD (1977) Enzyme clearing of alcian blue stained whole small vertebrates for demonstration of cartilage. *Stain Technology*, **52**, 229–232.
- Dittmar EL, Oakley CG, Conner JK, Gould B, Schemske D (2016) Factors influencing the effect size distribution of adaptive substitutions. *Proceedings of the Royal Society B*, **283**, 20153065.
- Ellegren H, Sheldon BC (2008) Genetic basis of fitness differences in natural populations. *Nature*, **452**, 169–75.
- Erickson DL, Fenster CB, Stenøien HK, Price D (2004) Quantitative trait locus analyses and the study of evolutionary process. *Molecular Ecology*, **13**, 2505–22.
- Erickson P, Glazer A, Cleves P, Smith A, Miller CT (2014) Two developmentally temporal quantitative trait loci underlie convergent evolution of increased branchial bone length in sticklebacks. *Proc. R. Soc. B*, **281**, 20140822.
- Erickson PA, Glazer A, Killingbeck E *et al.* (2016) Partially repeatable genetic basis of benthic adaptation in threespine sticklebacks. *Evolution*, **70**, 887–902.
- Erwin DH (2000) Macroevolution is more than repeated rounds of microevolution. *Evolution & Development*, **2**, 78–84.
- Erwin DH (2015) Novelty and innovation in the history of life. *Current Biology*, **25**, R930–R940.

Feder JL, Berlocher SH, Roethele JB *et al.* (2003) Allopatric genetic origins for sympatric host-plant shifts and race formation in *Rhagoletis*. *Proceedings of the National Academy of Sciences of the United States of America*, **100**, 10314–9.

Ferris KG, Barnett LL, Blackman BK, Willis JH (2016) The genetic architecture of local adaptation and reproductive isolation in sympatry within the *Mimulus guttatus* species complex. *Molecular Ecology*, **In press.**, doi: 10.1111/mec.13763.

Fishman L, Kelly AJ, Willis JH (2002) Minor quantitative trait loci underlie floral traits associated with mating system divergence in *Mimulus*. *Evolution; international journal of organic evolution*, **56**, 2138–2155.

Franchini P, Fruciano C, Spreitzer ML *et al.* (2014) Genomic architecture of ecologically divergent body shape in a pair of sympatric crater lake cichlid fishes. *Molecular Ecology*, **23**, 1828–45.

Fryer G, Iles T (1972) *Cichlid fishes of the great lakes of Africa*. FAO.

Gagnaire P-A, Pavey S a, Normandeau E, Bernatchez L (2013) The genetic architecture of reproductive isolation during speciation-with-gene-flow in lake whitefish species pairs assessed by RAD sequencing. *Evolution; international journal of organic evolution*, **67**, 2483–97.

Gavrilets S, Losos JB (2009) Adaptive radiation: contrasting theory with data. *Science (New York, N.Y.)*, **323**, 732–7.

Gifford D, Schoustra S, Kassen R (2011) The length of adaptive walks is insensitive to starting fitness in *Aspergillus nidulans*. *Evolution*, **65**, 3070–3078.

Givnish TJ, Sytsma KJ, Smith J *et al.* (1997) Molecular evolution and adaptive radiation in *Brocchinia* (Bromeliaceae: Pitcairnioideae) atop tepuis of the Guyana Shield. In: *Molecular evolution and adaptive radiation*, pp. 259–311. Cambridge University Press, Cambridge.

Glazer AM, Cleves PA, Erickson PA, Lam AY, Miller CT (2014) Parallel developmental genetic features underlie stickleback gill raker evolution. *EvoDevo*, **5**, 19.

Harmon LJ, Losos JB, Davies TJ *et al.* (2010) Early bursts of body size and shape evolution are rare in comparative data. *Evolution; international journal of organic evolution*, **64**, 2385–2396.

Hecht BC, Thrower FP, Hale MC, Miller MR, Nichols KM (2012) Genetic architecture of migration-related traits in rainbow and steelhead trout, *Oncorhynchus mykiss*. *G3*, **2**, 1113–27.

Heliconius Genome Consortium (2012) Butterfly genome reveals promiscuous exchange of mimicry adaptations among species. *Nature*, **487**, 94–8.

Hine E, Blows MW (2006) Determining the effective dimensionality of the genetic variance-covariance matrix. *Genetics*, **173**, 1135–44.

Hohenlohe PA, Bassham S, Etter PD *et al.* (2010) Population genomics of parallel adaptation in threespine stickleback using sequenced RAD tags. *PLoS Genetics*, **6**, e1000862.

Huerta-Sánchez E, Jin X, Asan *et al.* (2014) Altitude adaptation in Tibetans caused by introgression of Denisovan-like DNA. *Nature*, **512**, 194–7.

Jeffery WR (2008) Emerging model systems in evo-devo: cavefish and microevolution of development. *Evolution & Development*, **10**, 265–72.

Jones FC, Grabherr MG, Chan YF *et al.* (2012) The genomic basis of adaptive evolution in threespine sticklebacks. *Nature*, **484**, 55–61.

Keller I, Wagner CE, Greuter L *et al.* (2013) Population genomic signatures of divergent adaptation, gene flow and hybrid speciation in the rapid radiation of Lake Victoria cichlid fishes. *Molecular Ecology*, **22**, 2848–63.

Kelly JK (2009) Connecting QTLs to the G-matrix of evolutionary quantitative genetics. *Evolution; international journal of organic evolution*, **63**, 813–25.

Kirkpatrick M (2009) Patterns of quantitative genetic variation in multiple dimensions. *Genetica*, **136**, 271–84.

Kocher TD (2004) Adaptive evolution and explosive speciation: the cichlid fish model. *Nature reviews Genetics*, **5**, 288–98.

Korves TM, Schmid KJ, Caicedo AL *et al.* (2007) Fitness effects associated with the major flowering time gene FRIGIDA in *Arabidopsis thaliana* in the field. *The American Naturalist*, **169**, E141–E157.

Lamichhaney S, Berglund J, Almén MS *et al.* (2015) Evolution of Darwin’s finches and their beaks revealed by genome sequencing. *Nature*, **518**, 371–375.

Lamichhaney S, Han F, Berglund J *et al.* (2016) A beak size locus in Darwin’s finches facilitated character displacement during a drought. *Science*, **352**, 470–474.

Lemmon ZH, Bukowski R, Sun Q, Doebley JF (2014) The role of cis-regulatory evolution in maize domestication. *PLoS Genetics*, **10**, e1004745.

De León LF, Podos J, Gardezi T, Herrel A, Hendry AP (2014) Darwin’s finches and their diet niches: the sympatric coexistence of imperfect generalists. *Journal of Evolutionary Biology*, **27**, 1093–104.

Levis N, Pfennig D (2016) Evaluating “plasticity-first” evolution in nature: key criteria and empirical approaches. *Trends in ecology & evolution*.

Li H (2013) Aligning sequence reads, clone sequences and assembly contigs with BWA-MEM. *arXiv preprint arXiv*, **1303.3997**.

Li H, Handsaker B, Wysoker A *et al.* (2009) The Sequence Alignment/Map format and SAMtools. *Bioinformatics (Oxford, England)*, **25**, 2078–9.

Linnen CR, Poh Y-P, Peterson BK *et al.* (2013) Adaptive evolution of multiple traits through multiple mutations at a single gene. *Science (New York, N.Y.)*, **339**, 1312–6.

Liu RK, Echelle AA (2013) Behavior of the Catarina Pupfish (Cyprinodontidae: *Megupsilon*

aporus), a severely imperiled species. *The Southwestern Naturalist*, **58**, 1–7.

Louthan AM, Kay KM (2011) Comparing the adaptive landscape across trait types: larger

QTL effect size in traits under biotic selection. *BMC Evolutionary Biology*, **11**, 60.

Malinsky, Richard J. Challis AMT, Schiffels S *et al.* (2015) Genomic islands of speciation

separate cichlid ecomorphs in an East African crater lake. *Science*, **350**, 1493–1498.

Manceau M, Domingues VS, Linnen CR, Rosenblum EB, Hoekstra HE (2010) Convergence

in pigmentation at multiple levels: mutations, genes and function. *Philosophical*

Transactions of the Royal Society of London. Series B, Biological Sciences, **365**, 2439–

50.

Martin CH (2010) Unexploited females and unreliable signals of male quality in a Malawi

cichlid bower polymorphism. *Behavioral Ecology*, **21**, 1195–1202.

Martin CH (2012) Weak disruptive selection and incomplete phenotypic divergence in two

classic examples of sympatric speciation: Cameroon crater lake cichlids. *The American*

Naturalist, **180**, E90–E109.

Martin CH (2013) Strong assortative mating by diet, color, size, and morphology but limited

progress toward sympatric speciation in a classic example: Cameroon crater lake

cichlids. *Evolution*, **67**, 2114–23.

Martin CH (2016a) Context-dependence in complex adaptive landscapes: frequency and trait-

dependent selection surfaces within an adaptive radiation of Caribbean pupfishes.

Evolution, **70**, 1265–1282.

Martin CH (2016b) The cryptic origins of evolutionary novelty: 1000-fold faster trophic

diversification rates without increased ecological opportunity or hybrid swarm.

Evolution.

Martin CH, Crawford JE, Turner BJ, Simons LH (2016) Diabolical survival in Death Valley:

recent pupfish colonization, gene flow, and genetic assimilation in the smallest species

range on earth. *Proceedings of the Royal Society B: Biological Sciences*, **283**, 23–34.

Martin CH, Cutler JS, Friel JP *et al.* (2015) Complex histories of repeated colonization and hybridization cast doubt on the clearest examples of sympatric speciation in the wild.

Evolution, **69**, 1406–1422.

Martin CH, Feinstein LC (2014) Novel trophic niches drive variable progress towards ecological speciation within an adaptive radiation of pupfishes. *Molecular Ecology*, **23**, 1846–62.

Martin CH, Genner M (2009) A role for male bower size as an intrasexual signal in a Lake Malawi cichlid fish. *Behaviour*, **146**, 963–978.

Martin CH, Wainwright PC (2011) Trophic novelty is linked to exceptional rates of morphological diversification in two adaptive radiations of *Cyprinodon* pupfishes. *Evolution; international journal of organic evolution*, **65**, 2197–212.

Martin CH, Wainwright PC (2013a) A remarkable species flock of *Cyprinodon* pupfishes endemic to San Salvador Island, Bahamas. *Bulletin of the Peabody Museum of Natural History*, **54**, 231–240.

Martin CH, Wainwright PC (2013b) On the measurement of ecological novelty: scale-eating pupfish are separated by 168 my from other scale-eating fishes. *PloS one*, **8**, e71164.

Martin CH, Wainwright PC (2013c) Multiple fitness peaks on the adaptive landscape drive adaptive radiation in the wild. *Science (New York, N.Y.)*, **339**, 208–211.

Matuszewski S, Hermisson J, Kopp M (2015) Catch me if you can: adaptation from standing genetic variation to a moving phenotypic optimum. *Genetics*, **200**, 178–574.

McGuigan K, Chenoweth SF, Blows MW (2005) Phenotypic divergence along lines of genetic variance. *The American Naturalist*, **165**, 32–43.

Meyer RS, Purugganan MD (2013) Evolution of crop species: genetics of domestication and diversification. *Nature reviews. Genetics*, **14**, 840–52.

- Mezey JG, Houle D (2005) The dimensionality of genetic variation for wing shape in *Drosophila melanogaster*. *Evolution; international journal of organic evolution*, **59**, 1027–38.
- Miller CT, Beleza S, Pollen A a *et al.* (2007) cis-Regulatory changes in Kit ligand expression and parallel evolution of pigmentation in sticklebacks and humans. *Cell*, **131**, 1179–89.
- Miller CT, Glazer AM, Summers BR *et al.* (2014) Modular skeletal evolution in sticklebacks is controlled by additive and clustered quantitative trait loci. *Genetics*, **197**, 405–420.
- Mims MC, Darrin Hulsey C, Fitzpatrick BM, Streelman JT (2010) Geography disentangles introgression from ancestral polymorphism in Lake Malawi cichlids. *Molecular ecology*, **19**, 940–51.
- O’Quin CT, Drilea AC, Conte M a, Kocher TD (2013) Mapping of pigmentation QTL on an anchored genome assembly of the cichlid fish, *Metriaclima zebra*. *BMC genomics*, **14**, 287.
- Van Ooijen JW (2006) JoinMap ® 4, Software for the calculation of genetic linkage maps in experimental populations. *Kyazma BV, Wageningen*, **33**, 10–1371.
- Orr HA (1998) The population genetics of adaptation: the distribution of factors fixed during adaptive evolution. *Evolution*, **52**, 935–949.
- Orr HA (1999) The evolutionary genetics of adaptation. *Genetical Research*, **74**, 207–214.
- Orr HA (2005a) The genetic theory of adaptation: a brief history. *Nature reviews. Genetics*, **6**, 119–27.
- Orr HA (2005b) Theories of adaptation: what they do and don’t say. *Genetica*, **123**, 3–13.
- Ortíz-Barrientos D, Noor MAF (2005) Evidence for a one-allele assortative mating locus. *Science (New York, N.Y.)*, **310**, 1467.
- Parsons K, Concannon M, Navon D *et al.* (2016) Foraging environment determines the genetic architecture and evolutionary potential of trophic morphology in cichlid fishes.

Molecular Ecology, **In press**.

Parsons K, Taylor A, Powder K, RC A (2014) Wnt signalling underlies the evolution of new phenotypes and craniofacial variability in Lake Malawi cichlids. *Nature communications*, **5**.

Pennell M, Kirkpatrick M, Otto S, Vamosi J (2015) Y fuse? Sex chromosome fusions in fishes and reptiles. *PLoS*.

Peterson BK, Weber JN, Kay EH, Fisher HS, Hoekstra HE (2012) Double digest RADseq: an inexpensive method for de novo SNP discovery and genotyping in model and non-model species. *PloS one*, **7**, e37135.

Pfaender J, Hadiaty RK, Schliewen UK, Herder F (2016) Rugged fitness landscapes shape complex adaptive radiation. *Proc. R. Soc. B*, **283**, 23–42.

Protas ME, Hersey C, Kochanek D *et al.* (2006) Genetic analysis of cavefish reveals molecular convergence in the evolution of albinism. *Nature Genetics*, **38**, 107–11.

R Core Team (2015) R: A language and environment for statistical computing.

Recknagel H, Elmer KR, Meyer A (2013) A hybrid genetic linkage map of two ecologically and morphologically divergent Midas cichlid fishes (*Amphilophus* spp.) obtained by massively parallel DNA sequencing (ddRADSeq). *G3*, **3**, 65–74.

Reding DM, Foster JT, James HF, Pratt HD, Fleischer RC (2009) Convergent evolution of “creepers” in the Hawaiian honeycreeper radiation. *Biology letters*, **5**, 221–4.

Rieseberg LH, Kim S-C, Randell R a *et al.* (2007) Hybridization and the colonization of novel habitats by annual sunflowers. *Genetica*, **129**, 149–65.

Roberts RB, Hu Y, Albertson RC, Kocher TD (2011) Craniofacial divergence and ongoing adaptation via the hedgehog pathway. *Proceedings of the National Academy of Sciences of the United States of America*, **108**, 13194–13199.

Rockman M V. (2012) The QTN program and the alleles that matter for evolution: All that’s

gold does not glitter. *Evolution*, **66**, 1–17.

Rogers SM, Bernatchez L (2007) The genetic architecture of ecological speciation and the association with signatures of selection in natural lake whitefish (*Coregonus* sp.

Salmonidae) species pairs. *Molecular biology and evolution*, **24**, 1423–38.

Rogers SM, Tamkee P, Summers B *et al.* (2012) Genetic signature of adaptive peak shift in threespine stickleback. *Evolution*, **66**, 2439–2450.

Rohlf FJ (2001) Comparative methods for the analysis of continuous variables: geometric interpretations. *Evolution; international journal of organic evolution*, **55**, 2143–60.

Schindelin J, Arganda-Carreras I, Frise E *et al.* (2012) Fiji: an open-source platform for biological-image analysis. *Nature methods*, **9**, 676–82.

Schluter D (1996) Adaptive radiation along genetic lines of least resistance. *Evolution*.

Schluter D, Grant P (1984) Determinants of morphological patterns in communities of Darwin's finches. *American Naturalist*, **123**, 175–196.

Sen S, Satagopan J, Broman K, Churchill G (2007) R/qtlDesign: inbred line cross experimental design. *Mammal Genome*, **18**, 87–93.

Servedio MR, Van Doorn GS, Kopp M, Frame AM, Nosil P (2011) Magic traits in speciation: “magic” but not rare? *Trends in ecology & evolution*, **26**, 389–97.

Setiamarga DHE, Miya M, Yamanoue Y *et al.* (2008) Interrelationships of Atherinomorpha (medakas, flyingfishes, killifishes, silversides, and their relatives): The first evidence based on whole mitogenome sequences. *Molecular Phylogenetics and Evolution*, **49**, 598–605.

Shapiro MD, Kronenberg Z, Li C *et al.* (2013) Genomic diversity and evolution of the head crest in the rock pigeon. *Science*, **339**, 1063–7.

Stankowski S, Streisfeld MA (2015) Introgressive hybridization facilitates adaptive divergence in a recent radiation of monkeyflowers. *Proceedings of the Royal Society of*

London B, **282**, 20151666.

Stern DL, Orgogozo V (2009) Is genetic evolution predictable? *Science (New York, N.Y.)*, **323**, 746–51.

Stevenson MM (1981) Karyomorphology Of several species Of *Cyprinodon*. *Copeia*, **1981**, 494–498.

Turner BJ, Duvernell DD, Bunt TM, Barton MG (2008) Reproductive isolation among endemic pupfishes (*Cyprinodon*) on San Salvador Island, Bahamas: microsatellite evidence. *Biological Journal of the Linnean Society*, **95**, 566–582.

Wagner GP, Kenney-Hunt JP, Pavlicev M *et al.* (2008) Pleiotropic scaling of gene effects and the “cost of complexity”. *Nature*, **452**, 470–472.

Wagner GP, Zhang J (2011) The pleiotropic structure of the genotype-phenotype map: the evolvability of complex organisms. *Nature Reviews Genetics*, **12**, 204–13.

Weber JN, Peterson BK, Hoekstra HE (2013) Discrete genetic modules are responsible for complex burrow evolution in *Peromyscus* mice. *Nature*, **493**, 402–5.

Yeaman S, Whitlock MC (2011) The genetic architecture of adaptation under migration-selection balance. *Evolution*, **65**, 1897–1911.

Yong L, Peichel CL, McKinnon JS (2016) Genetic architecture of conspicuous red ornaments in female threespine stickleback. *G3*, **6**, 579–588.

Zhan S, Zhang W, Niitepold K *et al.* (2015) The genetics of monarch butterfly migration and warning coloration. *Nature*, **514**, 317–321.

Table 1. All 30 skeletal traits measured and sex, indicating maximum LOD score, linkage group (LG) associated with the maximum LOD score, maximum likelihood position within this linkage group and 95% Bayesian confidence interval, *P*-values, percent variance explained (PVE), number of phenotyped individuals, and available estimates of trait

diversification rates on San Salvador relative to outgroups for two comparative datasets: *a*) across Cyprinodontidae in bold (Martin & Wainwright 2011) and *b*) across Caribbean populations in italics (Martin 2016b)

. Note that significant QTL determined by permutation testing are highlighted in bold. Effect sizes illustrated in Fig. 6 and LOD profiles in Fig. 4, Fig. S2; morphometric landmarks for traits described in supplemental methods and illustrated in Fig. 3.

trait	max LOD	LG	position (cM) (95% CI)	<i>P</i>	PVE	<i>n</i>	relative diversification rate
sex	5.61	1	105 (88, 111.6)	2e-5	12.9	160	
premaxilla length	6.85	15	20.8 (13, 37.3)	5e-7	15.3	178	51.3 , <i>13.4</i>
premaxilla ventral arm width	5.47	15	35 (15, 41)	9e-6	12.3	180	<i>1.44</i>
lower jaw length	4.83	15	20.8 (5, 35)	5e-5	10.5	180	51.4 , <i>30.8</i>
dentigerous arm width	4.62	15	28 (7, 40)	1e-4	9.8	180	<i>4.7</i>
jaw closing in-lever	4.02	8	19 (4, 32)	1e-4	9.8	179	2.7 , <i>1.43</i>
palatine height	4.76	8	58.4 (33, 58.4)	1e-4	9.9	180	<i>4.5</i>
cranial height	4.11	2	21.2 (13, 26)	2e-4	9.0	180	<i>1.44</i>
caudal peduncle height	3.71	9	24 (0, 29)	1e-3	7.0	180	
maxillary head protrusion	3.17	16	19.5 (0, 29.1)	0.003	6.4	179	17.7 , <i>2.78</i>
maxilla length	3.44	8	25.7 (19, 58.4)	4e-4	8.5	179	17.1 , <i>2.59</i>
maxillary head height	3.22	3	87 (0, 87)	0.002	6.6	180	
premaxillary ascending process	2.15	5	69 (0, 72.1)	0.036	3.7	178	<i>1.39</i>
nasal tissue protrusion	2.71	15	45.1 (18, 48.6)	0.003	6.4	178	
anterior body depth	2.2	6	28.2 (12, 65.7)	0.009	5.2	179	2.2
posterior body depth	3.02	1	103 (63, 111.6)	0.004	6.0	179	
caudal peduncle length	2.96	1	27 (3, 99)	0.001	7.5	179	
dorsal fin height	3.12	18	31.6 (6, 44)	0.006	5.7	177	
dorsal fin length	3.19	23	25.9 (5, 30.2)	0.001	7.3	180	
anal fin height	2.47	20	39 (12.8, 42.5)	0.016	4.6	178	
anal fin length	1.72	18	45.7 (0, 45.7)	0.025	4.2	177	
cranium to dorsal fin	1.96	26	4 (5, 21)	0.024	4.1	179	
ectopterygiod	2.79	15	0 (0, 37)	0.009	5.2	180	
head depth	2.49	12	36 (18.2, 52.2)	0.004	6.0	180	<i>1.49</i>
cranium to pectoral girdle	3.68	21	4 (0, 14)	0.002	7.0	178	<i>1.17</i>
opening in-lever	2.19	5	55.9 (3, 71)	0.016	4.6	180	7.7 , <i>1.55</i>
orbit diameter	2.93	6	54.4 (0, 65.7)	0.006	5.5	180	0.3 , <i>1.2</i>
pelvic girdle length	2.23	7	61.5 (0, 61.5)	0.010	5.0	178	<i>2.93</i>
suspensorium length	3.23	6	56 (47, 65.7)	0.004	5.9	179	<i>2.12</i>
premaxilla to pectoral girdle	3.13	9	24 (9, 32)	0.002	6.8	179	
specimen size (SL)	1.75	15	45.1 (0, 48.6)	0.025	4.1	180	

Fig. 1

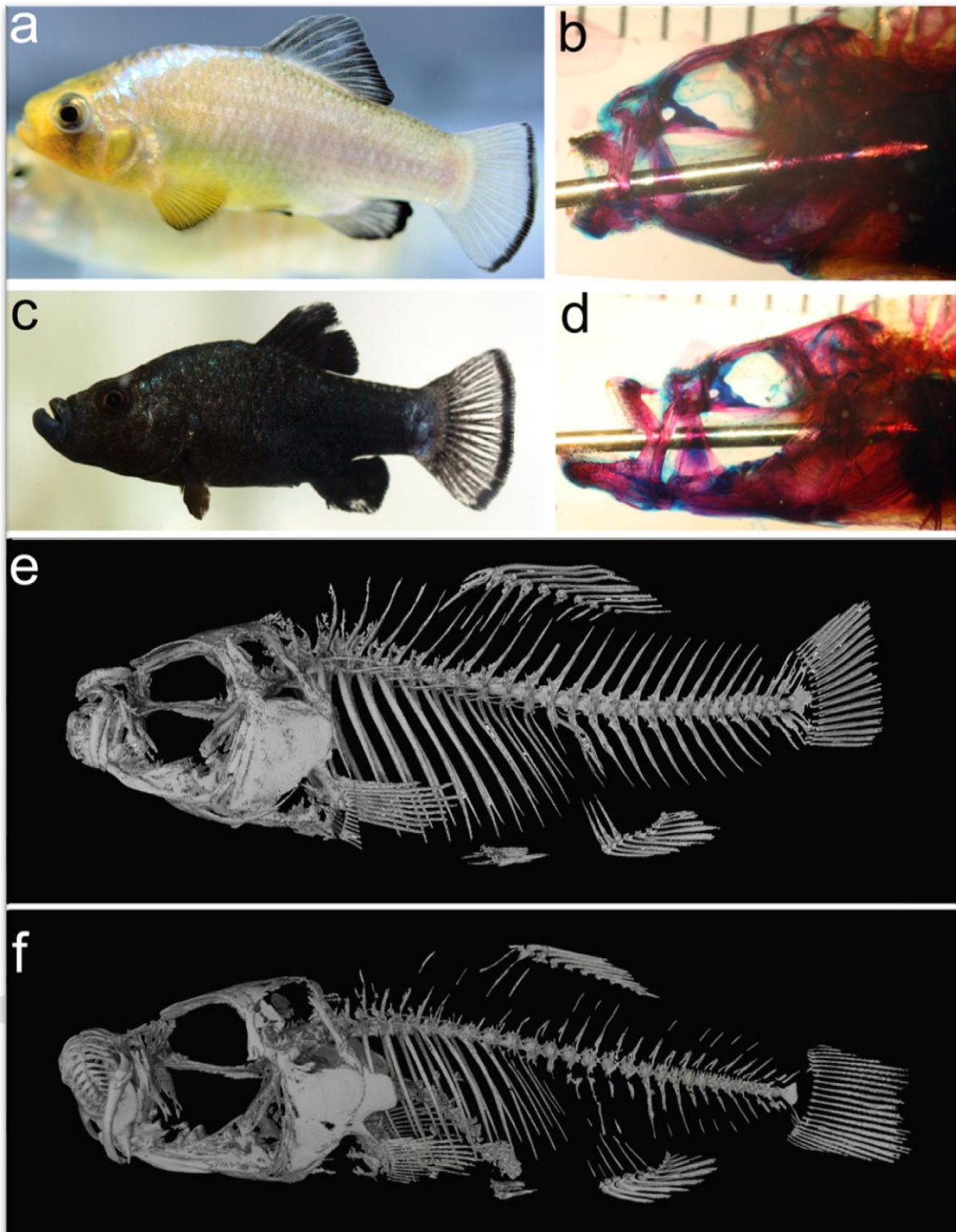


Fig. 1 Trophic specialist pupfish species endemic to San Salvador Island, Bahamas used for the F2 intercross. The molluscivore *Cyprinodon brontotheroides* (a-b,e) and scale-eater *C. desquamator* (c-d,f) are shown displaying their (a,c) representative male reproductive

coloration, (b,d) cleared and double-stained skeletal prep specimens, and e-f) μ CT scans of each species. Note the enlarged oral jaws of the scale-eater and nasal protrusion of the molluscivore (maxillary extension).

Fig. 2

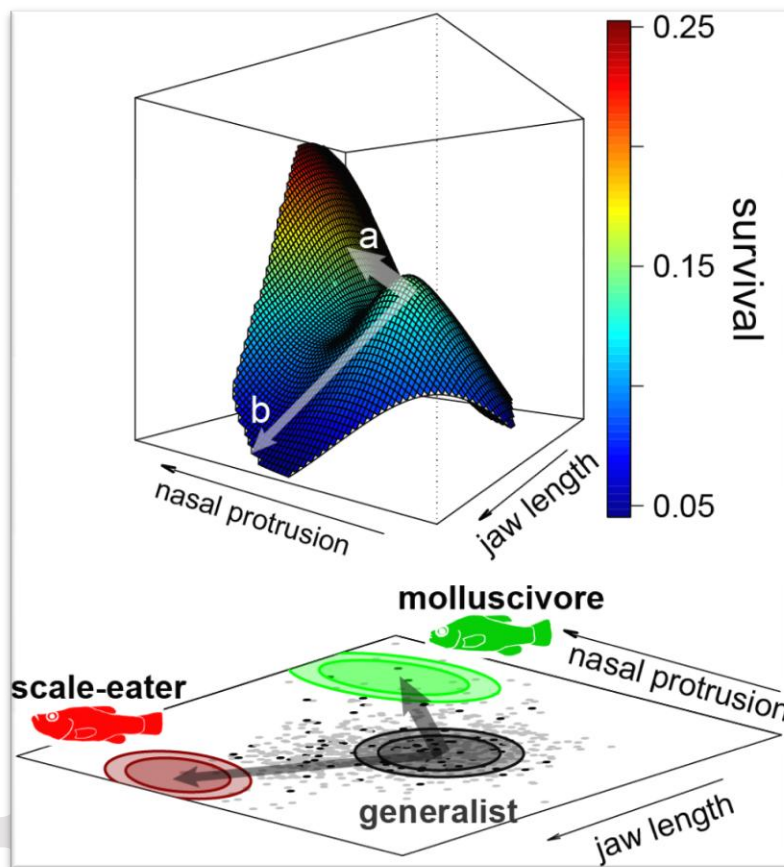


Fig. 2 Field measurements of the fitness landscape from F2 hybrid survival (black dots: survivors; grey dots: deaths) within a high-density field enclosure in Crescent Pond, San Salvador, Bahamas ($n = 796$ F2 hybrids; modified from Martin and Wainwright 2013c). F2 hybrids intercrossed and backcrossed to all 3 San Salvador species were raised in the lab to approximately 2 cm and photographed for phenotype measurements before tracking their survival in a 3 m field enclosure for 3 months as described previously (Martin and

Wainwright 2013c). *a*) A short, shallow fitness valley separates the ancestral generalist (grey ellipse) from a higher fitness peak corresponding to the molluscivore (green ellipse). *b*) A longer, deeper fitness valley isolates the scale-eater (red ellipse) with no detected fitness peak within the range of F2 hybrid phenotypes. Ellipses indicate 95% and 80% confidence intervals of the parental phenotypes plotted on the two discriminant axes (LD1: “jaw length”; LD2: “nasal protrusion”) separating the three parental species. The major traits differentiating the specialists, the enlarged oral jaws of the scale-eater and unique nasal protrusion of the molluscivore, load strongly on LD1 and LD2, respectively (see Table S3 in Martin and Wainwright 2013c), and exhibited the strongest loadings on the first and fourth principal components of hybrid variation which were also significantly associated with the survival of F2 hybrids (Martin and Wainwright 2013c: Table S5). Similarly, these two traits were strongly correlated with the first and second principal axes of nonlinear selection in projection pursuit regression (Martin and Wainwright 2013c: Table S6). Note that premaxilla length in this study corresponds to “craniofacial height” (external landmarks: jaw joint to tip of upper jaw) in (Martin and Wainwright 2013c) and nasal protrusion traits were “maxillary head protrusion” and “maxillary head protrusion angle”.

Fig. 3

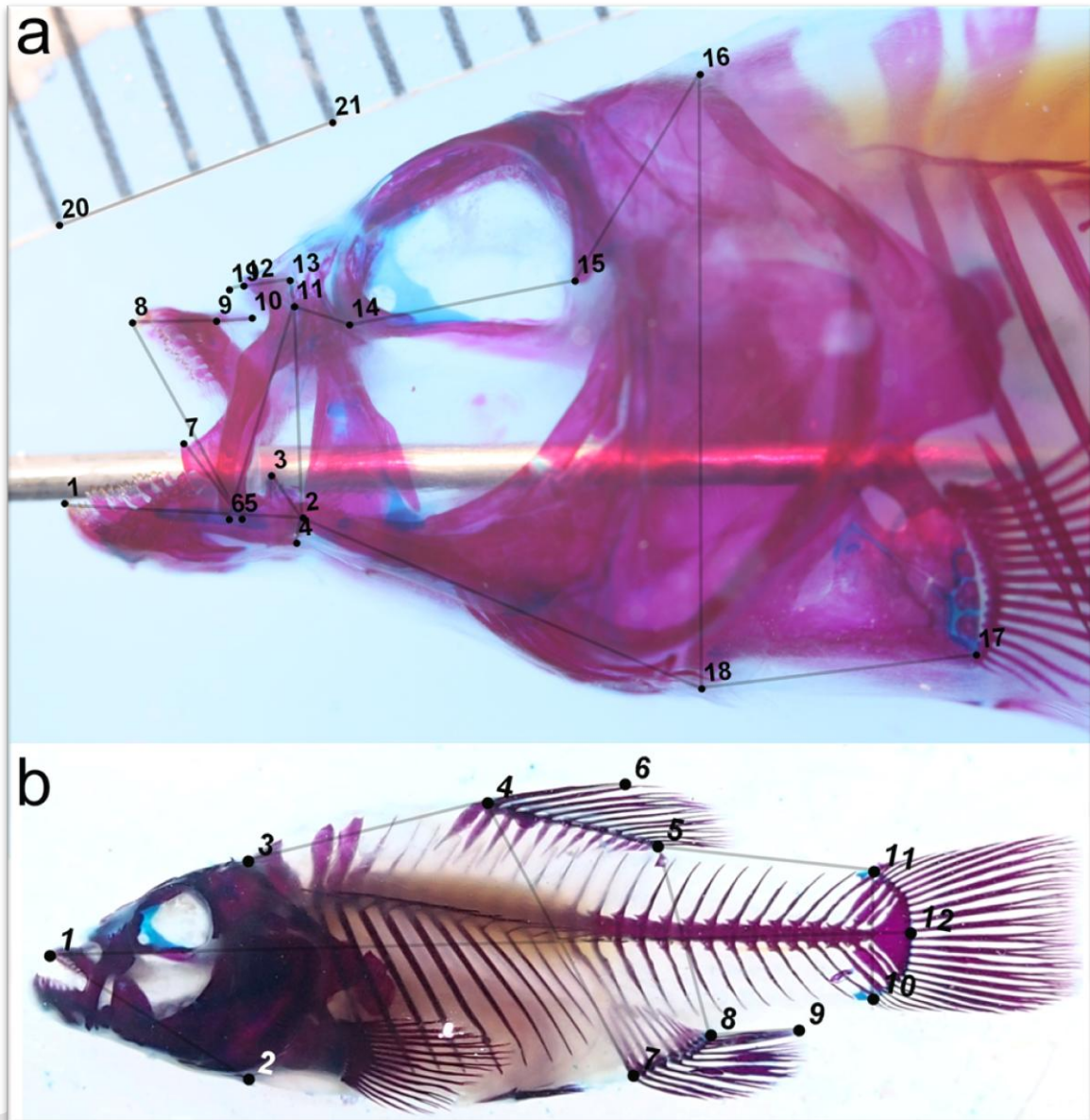


Fig. 3 Representative photographs of F2 intercross specimens showing landmarks used to measure linear distances among skeletal traits in lateral photographs of the *a*) head and pectoral girdle (19 landmarks plus two calibration points) with oral jaws adducted and *b*) whole body view (12 landmarks plus two calibration points). F2 intercross specimens were each suspended in glycerin after clearing and double staining with alizarin and alcian blue and photographed with a macro lens on both left and right sides. Images were calibrated with a 4mm grid or ruler.

Fig. 4

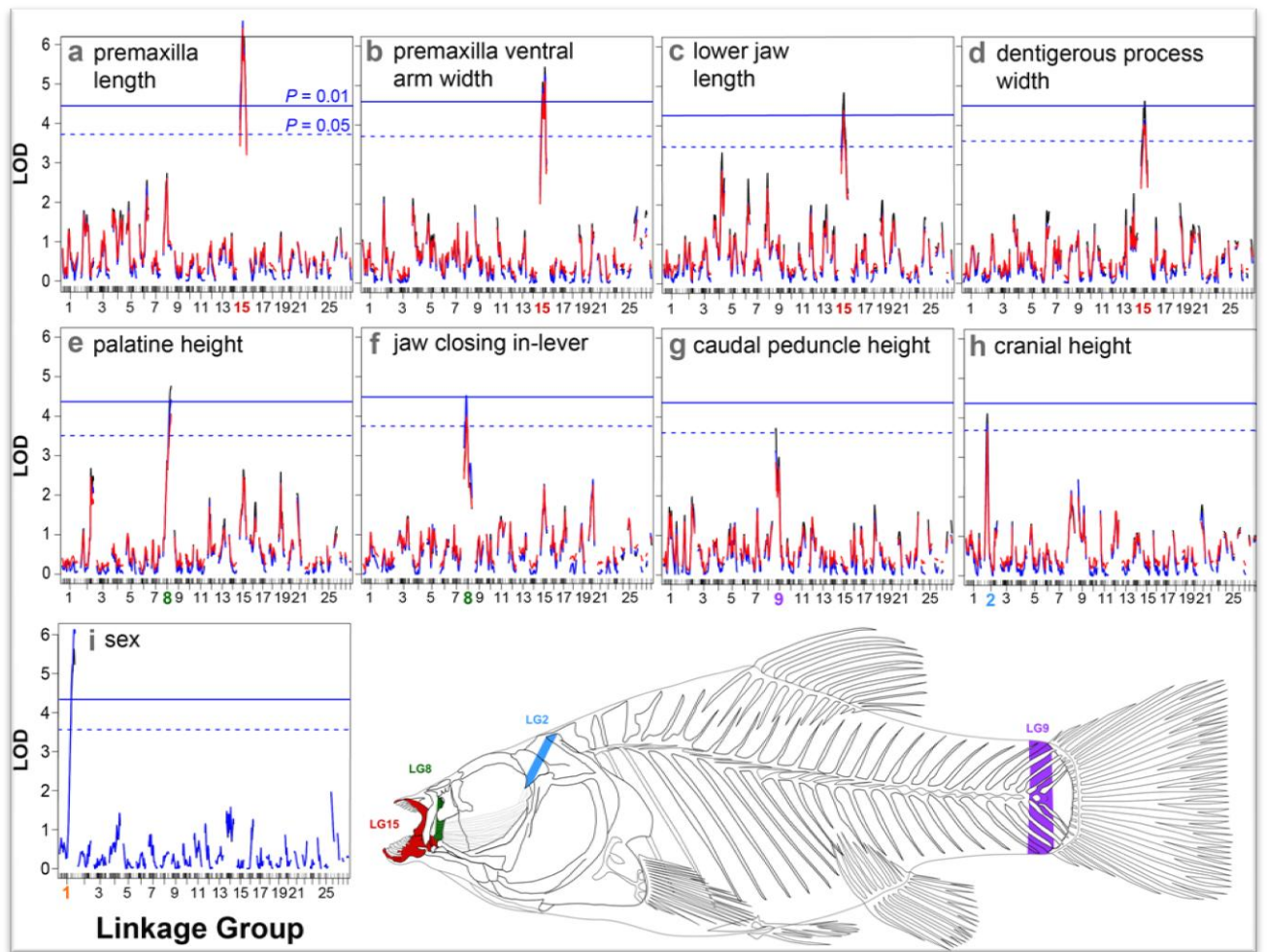


Fig. 4 Significant quantitative trait loci detected for *a-h*) eight skeletal traits and *i*) sex within a San Salvador pupfish F2 intercross. LOD profiles are plotted relative to position along the 29 linkage groups as estimated by Haley-Knott regression (black line), maximum likelihood (blue line), and multiple imputation (red line). Genome-wide significance levels of $P = 0.05$ (dotted blue line) and $P = 0.01$ (solid blue line) were calculated by permutation for each trait under the maximum likelihood model. Linkage groups significantly associated with traits are highlighted in bold colors and plotted on the skeletal *Cyprinodon* diagram; note that linkage groups 15 and 8 are associated with four and two traits, respectively. Multiple imputation was not available in binary trait models for sex in *i*.

Fig. 5

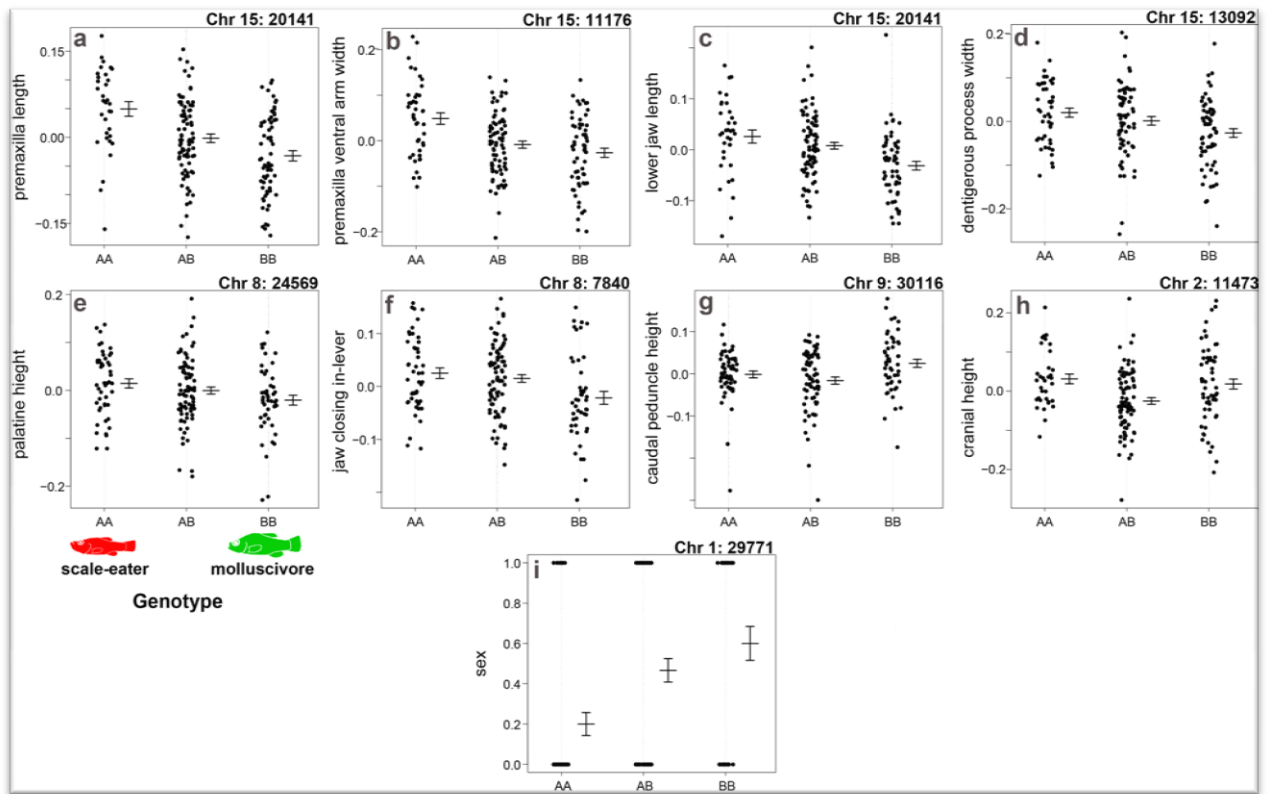


Fig. 5 Phenotype distribution relative to marker genotype for each significant QTL. For each skeletal trait, the AA genotype corresponds to the scale-eater grandparent (red) and the BB genotype corresponds to the molluscivore grandparent (green). Genetic marker locus ID is shown in the upper right corner of each plot, corresponding to Fig. 4 and the supplemental catalog of genetic markers. All skeletal traits (*a-h*) are size-corrected residuals from a log trait vs. log SL linear regression. For sex QTL: male = 1; female = 0.

Fig. 6

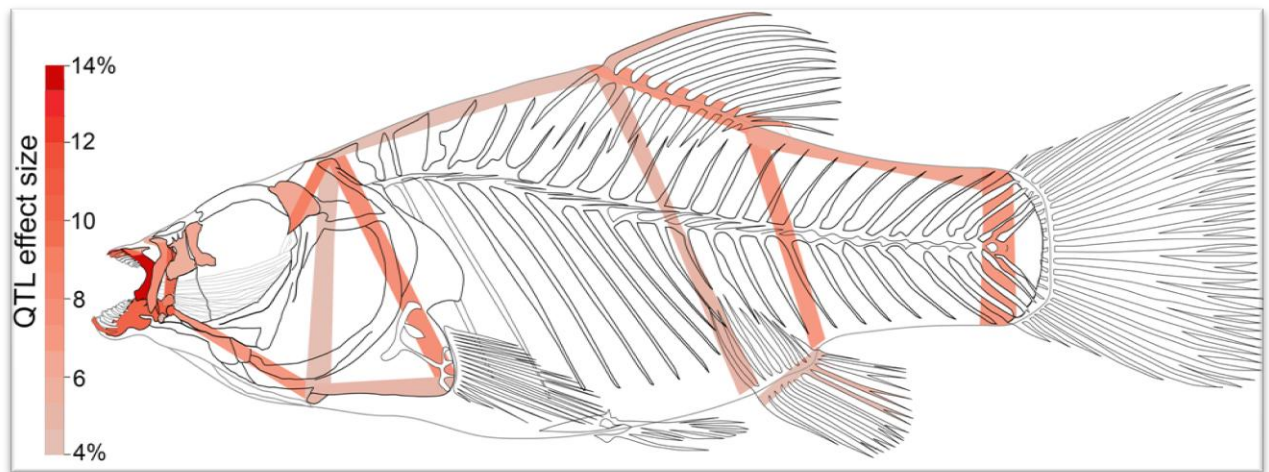


Fig. 6 *Cyprinodon* ‘morphogram’ with heat colors indicating the phenotypic variance explained (effect size) by the maximum likelihood QTL for each trait measured (Fig. 4-5, S2, Table 1). Note that the oral jaws are associated with larger effect size QTL in contrast to fin, head, and body size traits. All traits were measured as linear distances from lateral photographs of cleared and alizarin-stained specimens (Fig. 2). We caution that effect sizes below approximately 9% of phenotypic variance explained were associated with non-significant LOD scores (Table 1).